Reaction-diffusion model for the preparation of polymer gratings by patterned ultraviolet illumination

Reaction–diffusion model for the preparation of polymer gratings by patterned ultraviolet illumination

Christian M. Leewis,[a] Arthur M. de Jong, and Leo J. van IJzendoorn
Department of Applied Physics, Accelerator Laboratory, Eindhoven University of Technology, P.O. Box 513, 5600 MB Eindhoven, The Netherlands

Dirk J. Broer
Eindhoven Polymer Laboratories, Eindhoven University of Technology, P.O. Box 513, 5600 MB Eindhoven and Philips Research Laboratories, Prof. Holstlaan 4, 5656 AA Eindhoven, The Netherlands

(Received 8 December 2003; accepted 29 January 2004)

A model is developed to describe the migration mechanism of monomers during the lithographic preparation of polymer gratings by ultraviolet polymerization. The model is based on the Flory–Huggins theory: a thermodynamic theory that deals with monomer/polymer solutions. During the photoinduced polymerization process, monomer migration is assumed to be driven by a gradient in the chemical potential rather than the concentration. If the chemical potential is used as the driving force, monomer migration is not only driven by a difference in concentration, or volume fraction, but also by other entropic effects such as monomer size and the degree of crosslinking of the polymer network, which is related to the ability of a polymer to swell. Interaction of the monomers with each other or the polymer is an additional energetic term in the chemical potential. The theoretical background of the model is explained and results of simulations are compared with those of nuclear microprobe measurements. A nuclear microprobe is used to determine the spatial monomer distribution in the polymer gratings. It is shown that two-way diffusion is expected if the monomers are both difunctional and have the same size. In some cases, if one monomer is considerably smaller than the other, it can eventually have a higher concentration in the illuminated regions, even when it has a lower reactivity. The model is used to simulate the grating formation process. This results in a calculated distribution of the monomer volume fractions as a function of position in polymer gratings. An excellent agreement with the nuclear microprobe measurements is obtained. [DOI: 10.1063/1.1688458]

I. INTRODUCTION

Optical applications for functional polymers are found in data transport, storage and displays.[1–3] In this article polymer gratings are discussed. Essential for these devices is that they have some sort of distribution in either the refractive index or the film thickness. Patterned ultraviolet (UV) illumination is a technique that is used to prepare polymer structures having a modulation in monomer unit concentration from a homogeneous mixture of two monomers. Some regions are illuminated by UV light and polymerization is started, while other regions remain dark. If desired, one can vary the light intensity gradually. Monomer migration, induced by difference in properties of the monomers, during this polymerization process results in lateral differences in monomer concentration. If two monomers with an intrinsic difference in refractive index are used, these concentration modulations correspond directly to a modulation of the refractive index.

As shown in previous articles,[4,5] this monomer migration process depends on the differences in the properties of the monomers. First, when a monofunctional and a difunctional monomer are used, overall mass transport may occur, in which both monomers diffuse towards the illuminated regions. This is achieved by swelling of the growing, weakly crosslinked, polymer in the illuminated regions due to suction of monomers from the dark regions, while differences in other monomer properties such as the rate of consumption due to polymerization cause concentration variations. This mechanism describes the formation of a grating and shows variations in thickness, together with relative differences in the concentration of the monomers. Second, when two difunctional monomers are used, two-way diffusion, induced by differences in reactivity, describes the formation of a film with a constant thickness and variations of monomer unit concentrations. The more reactive monomer is depleted faster in the illuminated regions. This induces a concentration gradient that initiates a diffusion process, in which the more reactive monomer moves to the illuminated regions and the less reactive monomer moves to the dark regions. No swelling of the illuminated regions is observed, due to the crosslinking ability of the monomers. In literature, several models describing the diffusion of monomers in similar systems are found.[6,7] Other models in literature describe diffusion of reactive monomers in a polymer matrix.[8] However, these models predict that the most reactive monomer always migrates towards the regions of maximum UV intensity while earlier nuclear microprobe measurements on polymer

[a]Author to whom correspondence should be addressed; electronic mail: c.m.leewis@tue.nl

gratings[4,5] suggest otherwise. There, several gratings were prepared from combinations of 2-chloroethylacrylate, hexafluorobisphenol-'A'-diacrylate and 1,3-bis(3-methacryloxypropyl)-1,1,3,3-tetramethyldisiloxane, which are denoted further as Cl-monoacrylate, F-diacrylate, and Si-dimethacrylate, respectively. It was shown that, for a mixture of the Cl-monoacrylate and the F-diacrylate, the former had the higher final monomer unit concentration in the illuminated region despite its lower reactivity. Furthermore, thickness variations of 10%–25% between the illuminated and nonilluminated regions occur. These effects are not predicted by the models present in the literature.

When dealing with the reaction/diffusion process, the first thing one has to consider is that the driving force of monomer migration is the chemical potential of this monomer rather than its concentration. To find an expression for the chemical potential, it is necessary to consider the thermodynamics of mixing polymers and monomers. The Flory–Huggins theory[9–11] describes the thermodynamics of mixtures of polymers and solvents, polymers, and monomers and of two mutually different polymers. The theory yields expressions for the chemical potentials of monomers in mixtures with and without polymer, which can be utilized to model our grating formation. It further considers the degree of crosslinking of the polymer in relation to the urge to swell of a polymer network in solution, which is the situation in the illuminated regions. With these chemical potentials, it thus is possible to determine whether the liquid monomers flow to the illuminated or to the dark regions. However, an entropic term in this chemical potential related to the monomer size may play an important role in systems of two monomers of significantly different sizes. Monomer size and shape effects in the Flory–Huggins chemical potential are sometimes called ''size entropy''.[12] In the current article, it is shown that this may be the explanation why, in some cases, the less-reactive monomer is found to have the higher monomer unit concentration in the illuminated regions of the final structure.

In this article, a static and a dynamic reaction/diffusion model are presented that describe the grating preparation process incorporating monomer reactivity, monomer size, monomer crosslinking ability, surface tension, and diffusion coefficients as a function of the monomer conversion. With the model, it is possible to simulate the production of actual devices, which means that the monomer unit concentrations as a function of the position in the sample are simulated. These concentrations are compared with values that are determined experimentally with the nuclear microprobe.

II. EXPERIMENT

Cells for photopolymerization were prepared from two glass slides, one of which contained a patterned photomask consisting of different areas with grating periodicities ranging from 10 to 1000 μm. The cells are filled with the monomer mixture containing 0.1 wt % of photoinitiator (Irgacure 651). The samples were then illuminated through the photo mask by an UV light source (Philips PL10W/10 or TL-4W). Polymerization is initiated in the illuminated regions, which results in monomer migration. After the patterned illumination, the samples were turned over and illuminated uniformly, long enough to fix the film. The polymer gratings thus created were suitable for analysis.[4]

The samples were studied with a 3 MeV proton scanning microprobe with a spot size of about 12 μm.[5] Chlorine and silicon were detected by proton induced x-ray emission (PIXE), fluorine by proton induced gamma-ray emission (PIGE), and carbon and oxygen by Rutherford backscattering spectrometry (RBS). The detection angles and solid angles for PIXE and RBS were 135°, 18 msr and 147°, 11 msr, respectively. For PIGE, the detection angle is 90° and the solid angle times the efficiency is about 0.1 msr. In this way, the areal density, i.e., the mass per unit area of the film, of all elements, except hydrogen, is determined as a function of the position. More details about the microprobe analysis and a correction for ion beam induced damage are found in a previous article.[5] The monomer-unit concentration was determined as a function of the position in the sample.

Reaction rates of a number of mixing ratios of the different monomers were measured with differential scanning calorimetry (DSC) with a Perkin–Elmer Photo-DSC 7 with shutter control under nitrogen atmosphere. Oxygen inhibition of the initiation, i.e., the photoinitiator reacts first with oxygen instead of the monomers, was therefore reduced, resulting in an earlier start of the reaction and less photoinitiator depleted by the oxygen compared to the situation of the grating preparation process. The intensity of the UV light source was 2 mW/cm^2 at a wavelength of 370 nm. The photoinitiator (Irgacure 651) concentration was 0.5 mass % for all samples. The temperature was either $T=25$ or 65 °C, which corresponds to the temperatures used in the grating preparation process.

The sample and a reference sample were kept at a constant temperature during the whole experiment. For the first minute, a shutter was kept in front of the UV light source. After $t=1$ min, both the sample and the reference sample were irradiated with the UV light source. After exposure, the shutter was closed and eventual shifts in the baseline were checked for 1 min. During the experiment, the difference in heat flow rate to keep both samples at the same temperature was measured. This heat then corresponds to the heat released during polymerization. All graphs in this chapter were corrected for a baseline, which were determined from DSC calibration measurements of the polymerized material.[13] This was done for the same time as the measurement itself to ease comparison between the two measurements.

III. THEORY

First, a static reaction/diffusion model is explained, which shows the thermodynamic basis of the driving force for diffusion. The theoretical description of the model for the preparation of polymer gratings is explained. Two cases are considered: a one monomer and a two monomer system. Second, a dynamic model is developed that refines the static model with real values of reaction rate constants, diffusion coefficients and additional effects.

A. The static model

1. One monomer

In the case of a system of only one monomer, only two components have to be considered, i.e., the monomer and the polymer. The system is divided into an illuminated and a dark region. The monomer chemical potentials at a certain time in the polymerization process in both the illuminated and the dark region are given by Refs. 9 and 11, assuming a constant temperature, a constant ambient pressure, and a constant total volume of the system

$$\mu_1^{\text{illum}}-\mu_1^0=kT\left[\ln(1-\varphi_p^{\text{illum}})+\varphi_p^{\text{illum}}-\frac{\nu_1}{\nu_p}\varphi_p^{\text{illum}}+\chi_{1p}(\varphi_p^{\text{illum}})^2\nu_1+\nu_1\frac{n_e}{N_p}\left(\frac{1}{\varphi_p^{\text{illum}}}-\frac{\varphi_p^{\text{illum}}}{2}\right)\right], \tag{1}$$

$$\mu_1^{\text{dark}}-\mu_1^0=0. \tag{2}$$

Here, μ_1^0 is the chemical potential of an unmixed phase of monomer 1 and φ_p is the volume fraction of the polymer. Here, $\varphi_p=1-\varphi_1$, with φ_1 the monomer 1 volume fraction. The number of segments of the monomer and the polymer molecules are given by ν_1 and ν_p, respectively. Here, a segment is a volume unit that corresponds to the smallest monomer unit in the system, and should not be confused with a monomer unit in general in a system that contains monomers of different sizes. χ_{1p} is the Flory–Huggins interaction parameter, which accounts for energetic interaction between segments. The effective number of internal chains (i.e., between two crosslinks) is given by n_e, and is twice the effective number of crosslinks,[9] since in an ideal network each crosslink corresponds to four chain ends. N_p is the total number of segments of the (dry) polymer. n_e/N_p can thus be regarded as twice the crosslink density. The last term of Eq. (1) can be derived assuming swelling of the polymer is allowed only in the z direction.[11,14] In the literature, it is discussed whether the factor of 1/2 should be removed[15] in the last term or not.[16] For the basic ideas of the theory, this is of minor importance.

The third term within the brackets can be left out, since the number of segments of the monomers is far less than the number of segments of the polymer chains, so $\nu_1 \ll \nu_p$. In the case of a free-radical chain-addition polymerization this is even true in the very early stages of polymerization, since the full polymer chain is formed in a time fragment much smaller than the total polymerization time. For now, all interaction parameters are taken zero. So, $\chi_{1p}=0$. This seems especially reasonable since the solvent is the monomer of the very same polymer. Now Eqs. (1) and (2) become

$$\mu_1^{\text{illum}}-\mu_1^0=kT\left[\ln(1-\varphi_p^{\text{illum}})+\varphi_p^{\text{illum}}+\nu_1\frac{n_e}{N_p}\left(\frac{1}{\varphi_p^{\text{illum}}}-\frac{\varphi_p^{\text{illum}}}{2}\right)\right], \tag{3}$$

$$\mu_1^{\text{dark}}-\mu_1^0=0. \tag{4}$$

There is thermodynamic equilibrium if the monomer chemical potentials are the same in both the illuminated and the dark regions. If this is not the case, migration of the monomer occurs in principle until thermodynamic equilibrium is established. If there are no crosslinks, the last term of Eq. (3) equals zero ($n_e=0$). For any value of φ_p, in the absence of crosslinks, thermodynamic equilibrium is approached by migration of all monomer to the illuminated regions. For a nonzero crosslink density, the equilibrium value of φ_p can be calculated for given n_e and monomer diffusion would cause as much as possible monomer to migrate from the dark to the illuminated regions, to obtain this equilibrium volume fraction.

Two assumptions apply. First, it is assumed that there are no changes in volume of segments, which means that a monomer unit has the same volume whether it is polymerized or not. Polymer swelling at a certain position can therefore only occur when there is a net increase in the number of monomer units at that position. Second, it is assumed that the polymer is homogeneously mixed even for very dilute polymer solutions, although then the polymer segments are not distributed homogeneously. These assumptions, however, are not expected to have a significant effect for the overall process.

Interestingly, if n_e/N_p were given by the expression below, the chemical potentials would already be equal on both the liquid side and the mixed side, and no monomer diffusion would take place. Then, there is no net gain in mass in the illuminated regions and no swelling is possible

$$\frac{n_e}{N_p}=\frac{1}{\nu_1}\frac{-\ln(1-\varphi_p^{\text{illum}})-\varphi_p^{\text{illum}}}{\left(\frac{1}{\varphi_p^{\text{illum}}}-\frac{\varphi_p^{\text{illum}}}{2}\right)}. \tag{5}$$

2. Two monomers

When a grating is prepared[4] from a mixture of two monomers, three components have to be considered, i.e., the two monomers and the polymer, even though the composition of the polymer depends on the position in the sample and the reaction time. Following again the Flory–Huggins theory, the chemical potential μ_1^{illum} of monomer 1 is given by the following expressions:[9]

$$\mu_1^{\text{illum}}-\mu_1^0=kT\left[\ln\varphi_1^{\text{illum}}+1-\varphi_1^{\text{illum}}-\frac{\nu_1}{\nu_2}\varphi_2^{\text{illum}}-\frac{\nu_1}{\nu_p}\varphi_p^{\text{illum}}+(\chi_{12}\varphi_2^{\text{illum}}+\chi_{1p}\varphi_p^{\text{illum}})\times(\varphi_2^{\text{illum}}+\varphi_p^{\text{illum}})\nu_1-\chi_{2p}\nu_1\varphi_2^{\text{illum}}\varphi_p^{\text{illum}}+\nu_1\frac{n_e}{N_p}\left(\frac{1}{\varphi_p^{\text{illum}}}-\frac{\varphi_p^{\text{illum}}}{2}\right)\right]. \tag{6}$$

In a similar way μ_2^{illum} is found by exchanging indices 1 and 2. Here, μ_1^0 and μ_2^0 are the chemical potentials of the unmixed phases of monomer 1 and 2, respectively; and φ_1,

φ_2, and φ_p are the volume fraction of monomer 1, monomer 2, and the polymer respectively. $\varphi_p^{\text{illum}}+\varphi_1^{\text{illum}}+\varphi_2^{\text{illum}}=1$ and $\varphi_1^{\text{dark}}+\varphi_2^{\text{dark}}=1$, always. The number of segments of the different monomers, as defined in the Flory–Huggins model, is given by ν_1 and ν_2, respectively. Interestingly, since the number of segments is directly related to the size or length of the monomer, there is a length or size dependent factor ν_1/ν_2. This factor is sometimes called size entropy.[12]

In the case of mixing two ideal gases or some other hard spheres, the chemical potential μ is given by $\mu=kT\ln c$ with c the number concentration. This expression can be derived from the Flory–Huggins expression given by Eq. (6) assuming zero interaction, $\chi_{ij}=0$, no crosslinking, $n_e=0$, and molecules with equal sizes, $\nu_1=\nu_2$. In this case, concentrations and volume fractions are equal for both.

It should be emphasized that the Flory–Huggins treatment, involving this size entropy is not generally valid. It is only a valid approximation in the case rod shaped, flexible solvent, or monomer molecules are involved, and will be not valid in the case of globular molecules. However, since the monomers treated here have a elongated conformation rather than a spherical one, the approach sketched here is justified. In literature,[12] the size entropy is discussed in terms of steric interference rather than a difference in monomer size. However, the longer the molecule, the more steric interference occurs.

In the dark regions, the chemical potential for monomer 1 is defined as follows:

$$\mu_1^{\text{dark}}-\mu_1^0=kT\left[\ln\varphi_1^{\text{dark}}+1-\varphi_1^{\text{dark}}-\frac{\nu_1}{\nu_2}\varphi_2^{\text{dark}}+\chi_{12}(\varphi_2^{\text{dark}})^2\nu_1\right]. \tag{7}$$

Again, μ_2^{dark} is found in a similar way by exchanging the indices 1 and 2.

As before, the term involving ν_p can be ignored in Eq. (6), since the number of segments of the monomers is far less than the number of segments of the polymer, so $\nu_1\ll\nu_p$ and $\nu_2\ll\nu_p$. For now, all interaction parameters are taken zero; $\chi_{12}=\chi_{1p}=\chi_{2p}=0$. This assumption may not be valid because the monomers can have different interactions with itself and the polymer. In addition, the polymer consists of two types of monomer units, and it may not be justified to treat it with one interaction parameter. However, in the systems considered here, the polymer is made of its own monomer solvent. In addition, the monomer unit ratio in the polymer is usually not more than 10% different from the monomer ratio in the monomer mixture, which reduces the effect of any interaction driven migration.[4,5]

In the two-monomer case, the difference between the chemical potentials for monomer 1 between the dark and the illuminated regions can be derived by subtracting Eqs. (7) and (6)

$$\mu_1^{\text{dark}}-\mu_1^{\text{illum}}=kT\left[\ln\varphi_1^{\text{dark}}+1-\varphi_1^{\text{dark}}-\frac{\nu_1}{\nu_2}\varphi_2^{\text{dark}}-\ln\varphi_1^{\text{illum}}-1+\varphi_1^{\text{illum}}+\frac{\nu_1}{\nu_2}\varphi_2^{\text{illum}}-\nu_1\frac{n_e}{N_p}\left(\frac{1}{\varphi_p^{\text{illum}}}-\frac{\varphi_p^{\text{illum}}}{2}\right)\right]. \tag{8}$$

In the case where there is no network, the last term equals zero. Of course, $\mu_1^{\text{dark}}-\mu_1^{\text{illum}}$ increases when the volume fraction of monomer 1 in the dark regions φ_1^{dark} becomes larger, or if the volume fraction of monomer 2 in the dark regions, φ_2^{dark} becomes smaller. The driving force for flow of monomer 1 from the dark towards the illuminated regions then increases, since it is proportional to $\mu_1^{\text{dark}}-\mu_1^{\text{illum}}$.

Interestingly, if the size of molecule 1, ν_1, decreases, $-(\nu_1/\nu_2)\varphi_2^{\text{dark}}+(\nu_1/\nu_2)\varphi_2^{\text{illum}}$ becomes larger because φ_2^{dark} is higher than φ_2^{illum}; i.e., the monomer 2 volume fraction is higher in the dark regions than in the illuminated regions because $\varphi_p^{\text{illum}}+\varphi_1^{\text{illum}}+\varphi_2^{\text{illum}}=1$ and $\varphi_1^{\text{dark}}+\varphi_2^{\text{dark}}=1$. The result is that $\mu_1^{\text{dark}}-\mu_1^{\text{illum}}$ becomes larger. Therefore, the smaller the monomer size, the higher the equilibrium monomer 1 volume fraction in the illuminated regions becomes. If there is a network, things become slightly more difficult due to the extra network term that will increase the chemical potential in the illuminated regions and reduce the flow of monomer towards the illuminated regions. However, if the monomer 1 size decreases, again $\mu_1^{\text{dark}}-\mu_1^{\text{illum}}$ increases.

Summarizing, two effects contribute to a difference in chemical potential and therefore a flow of monomers towards the illuminated regions. First, there are concentration gradients. Intuitively, the higher the concentration gradient, the higher the driving force for migration. Second, the flow of monomers to the illuminated regions also increases if their molecular size decreases. The numerical procedure used to calculate the migration by the static reaction/diffusion model is displayed in Fig. 1 and explained in detail in Appendix A.

B. The dynamic reaction/diffusion model

In order to obtain a dynamic reaction/diffusion model, the diffusion laws need to be incorporated. Diffusion processes are often described with Fick's well-known second law. One assumes that the total volume of the system is constant. The flux of particles J ($\text{s}^{-1}\,\text{m}^{-2}$) is taken proportional to the concentration gradient of a species and applying conservation of mass results in Fick's second law

$$\frac{\partial c}{\partial t}=-\frac{\partial}{\partial x}J=\frac{\partial}{\partial x}\left(D\frac{\partial c}{\partial x}\right). \tag{9}$$

Here, J is the flux of particles, D the diffusion coefficient, c (m^{-3}) the concentration, and x the spatial parameter.

One should bear in mind that this is an empirical law and that, in general, a concentration gradient is not the driving force for diffusion. The real driving force is a gradient in the chemical potential. The flux of particles ($\text{s}^{-1}\,\text{m}^{-2}$) is then proportional to a gradient in the chemical potential[17,18] and the general diffusion equation becomes

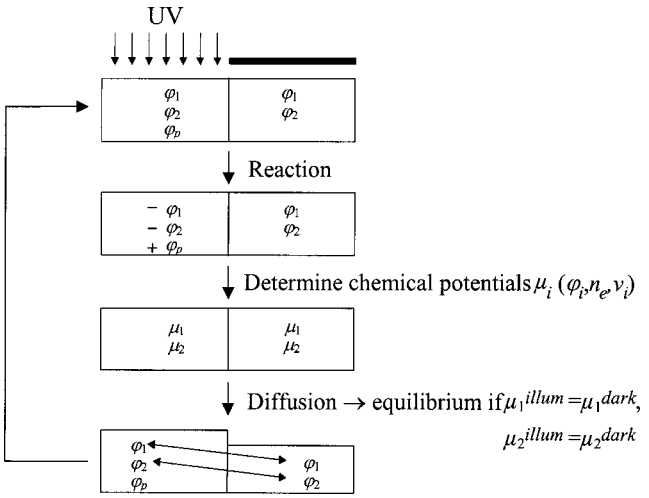

FIG. 1. A schematic representation of the static model. First, a certain volume of the monomers is converted into polymer according to their reactivity ratio. Then, their chemical potentials are determined. Then, the monomers are redistributed to re-establish thermodynamic equilibrium. The process is then repeated, until a certain conversion is achieved.

$$\frac{\partial c}{\partial t} = -\frac{\partial}{\partial x} J = \frac{\partial}{\partial x}\left(\frac{Dc}{kT}\frac{\partial \mu}{\partial x}\right). \tag{10}$$

If the total volume is a function of x and/or volume changes are allowed, conservation of mass demands that one cannot simply use the concentration. The concentration c should then be replaced by the volume of the migrating species per unit x.

As the polymerization proceeds, the monomer diffusion coefficients will drop, not only because of growing polymer chains but also because the crosslinking network increasingly hinders monomer diffusion. The diffusion coefficients can easily drop by 5 orders of magnitude[19] when going from a polymer volume fraction of 0 to 1.

With the free volume theory,[20,21] which treats the looseness of a polymer solution by means of an extra available volume,[22] the diffusion coefficient as a function of monomer concentration is given by

$$\left(\ln\frac{D(\varphi_m)}{D_p}\right)^{-1} = K_1\left(\frac{1}{\varphi_m} + K_2\right). \tag{11}$$

Here, φ_m is the monomer volume fraction, D_p is the monomer diffusion coefficient for $\varphi_m = 0$, i.e., in the pure polymer, and K_1 and K_2 are positive constants described in the free volume theory.[20,21]

As a result of the diffusion of monomers, a net overall transport of liquid monomer can occur. In the case of swelling of the illuminated regions, both monomers flow towards the illuminated regions and the amount of monomers in the dark regions decreases. The remaining monomer liquid is expected to redistribute itself in such a way that the surface of the monomer is at a minimum. This process can be driven by a hydrostatic pressure difference.[23] Strictly speaking, there is thermodynamic equilibrium between the solution in the illuminated regions and the pure liquid in the dark regions when the difference in the chemical potential is equal to the difference in pressure, i.e., $(\mu_1^{\text{dark}} - \mu_1^{\text{illum}}) = \nu_1 \nu_{\text{segment}} \Delta p$. Here, Δp is the difference in hydrostatic pressure between the solution in the illuminated regions and the pure liquid in the dark regions. However, since the difference in height of the illuminated and dark regions is only at most 30 μm, this pressure difference is ignored. Even if the glass slides[4] are firmly clamped, the effect of an extra pressure on the illuminated regions only plays a minor role.

The second driving force is the minimization of the surface tension of the film. To incorporate this in the model, a concept is adopted from the description of surface diffusion on solids.[24] There, the chemical potential of a surface is given by

$$\mu_s = -\kappa\gamma\nu = -\gamma\nu\frac{\dfrac{\partial^2 h}{\partial x^2}}{\left(1+\left(\dfrac{\partial h}{\partial x}\right)^2\right)^{3/2}}. \tag{12}$$

Here κ is the surface curvature,[25] γ the surface tension, and ν the molecular volume of the migrating species. The surface tension is about 0.030–0.040 J/m^2 for various (poly)(meth)acrylates.[26] For siloxane diacrylates it may even be lower. For the model, however, a value of 0.035 J/m^2 is used for every monomer mixture. Bulk migration, with n the number of migrating species per unit length in the x-direction, is then given by

$$\frac{\partial n}{\partial t} = -\frac{\partial}{\partial x} J = \frac{\partial}{\partial x}\left[\frac{D_s n}{kT}\frac{\partial \mu_s}{\partial x}\right]. \tag{13}$$

It should be noted that this migration only redistributes the total volume since it is assumed to work on both monomers equally. Any effect due to a difference in surface tension for these two monomers and the effect of the glass substrate is ignored. In fact, this diffusion can be interpreted as bulk flow compensating for differences in intrinsic diffusion coefficients of the two monomers used. A step-by-step description is given in Table I. A full description of the numerical procedure is found in Appendix B.

C. Results of the static model

In this section, three case studies of different combinations of 1:1 volume ratio mixtures of two monomers are considered. The probability to react, of monomer 2 is twice the reactivity of monomer 1, i.e., $R_2 = 2R_1$. The crosslinking ability f, as described in Appendix A, and the size ν are varied as described in Table II.

The first case study (case I) concerns a 1:1 volume ratio of a mono(meth)acrylate ($f_1 = 0$) and a di(meth)acrylate monomer ($f_2 = 1$), which are equal in size, i.e., $\nu_1 = \nu_2 = 1$. Thus initially, $\varphi_1^{\text{illum}} = \varphi_1^{\text{dark}} = 0.5$ and $\varphi_2^{\text{illum}} = \varphi_2^{\text{dark}} = 0.5$ and $V^{\text{dark}} = V^{\text{illum}} = V_0$. Assume that $0.15V_0$ of polymer is formed in the illuminated region during the first reaction step. Since $R_2 = 2R_1$, and the initial volume ratio is equal, the polymer

TABLE I. Step-by-step description of the dynamic reaction/diffusion model.

1	Conversion of monomer to polymer in illuminated regions only during a time interval of Δt according to reaction speeds; determine the new volumes of the monomers and the polymer in all regions of length Δx which are illuminated [Eqs. (B1), (B2)]; dark regions remain unchanged.
2	Determine the crosslink density in all regions of length Δx [Eq. (B7)].
3	Determine the chemical potential of both monomers in all regions of length Δx. [Eqs. (B3), (B4)].
4	Determine the diffusion coefficients of both monomers in all regions of length Δx since these depend on the polymer volume fraction [Eq. (B8)].
5	Diffusion process with the gradient in chemical potential of both monomers and the diffusion coefficients; determine the new volumes of monomers in all regions of length Δx during a time interval of Δt [Eq. (B9)]; absolute polymer volumes remain unchanged.
6	Determine the surface chemical potential in all regions of length Δx [Eq. (B10)].
7	Overall diffusion process according to the gradient in surface chemical potential; determine the new volumes of monomers in all regions of length Δx during a time interval of Δt [Eq. (B11)].
8	Go back to step 1.

Afterwards the grating is fixed. Here, it is simply assumed that all remaining monomer is converted into polymer, instantly without any diffusion.

consists of $0.05V_0$ of monomer 1 and $0.10V_0$ of monomer 2. Consequently,

$$\begin{aligned} &\varphi_{p,1}^{\text{illum}}=0.05, \quad \varphi_{p,2}^{\text{illum}}=0.10,\\ &\varphi_1^{\text{illum}}=0.45, \quad \varphi_2^{\text{illum}}=0.40,\\ &\varphi_1^{\text{dark}}=0.50, \quad \varphi_2^{\text{dark}}=0.50,\\ &V^{\text{illum}}=V^{\text{dark}}=V_0. \end{aligned} \tag{14}$$

With Eqs. (6) and (7), $\chi_{ij}=0$, $\nu_i/\nu_p=0$, $f_1=0$, $f_2=1$, the current chemical potentials are thus found to be

$$\frac{\mu_1^{\text{illum}}-\mu_1^0}{kT}=-0.640 \quad \frac{\mu_1^{\text{dark}}-\mu_1^0}{kT}=-0.693 \tag{15}$$

$$\frac{\mu_2^{\text{illum}}-\mu_2^0}{kT}=-0.758 \quad \frac{\mu_2^{\text{dark}}-\mu_2^0}{kT}=-0.693. \tag{16}$$

It is seen that the chemical potential of monomer 1 is higher in the illuminated regions and that the chemical potential of monomer 2 is higher in the dark regions. This implies that the volume fraction of monomer 1 is too high in the illuminated region and too low in the dark region. Solving Eqs. (6) and (7) for thermodynamic equilibrium, i.e., redistributing the mobile monomers, results in

$$\frac{\mu_1^{\text{illum}}-\mu_1^0}{kT}=\frac{\mu_1^{\text{dark}}-\mu_1^0}{kT}=-0.666, \tag{17}$$

$$\frac{\mu_2^{\text{illum}}-\mu_2^0}{kT}=\frac{\mu_2^{\text{dark}}-\mu_2^0}{kT}=-0.721, \tag{18}$$

$$\begin{aligned} &\varphi_1^{\text{illum}}=0.446, \quad \varphi_2^{\text{illum}}=0.422,\\ &\varphi_{p,1}^{\text{illum}}=0.044, \quad \varphi_{p,2}^{\text{illum}}=0.088,\\ &\varphi_1^{\text{dark}}=0.513, \quad \varphi_2^{\text{dark}}=0.486,\\ &V^{\text{illum}}=1.138V_0, \quad V^{\text{dark}}=0.862V_0. \end{aligned} \tag{19}$$

The ratio of the volume fractions of unreacted monomer 1 to unreacted monomer 2 is equal for both regions. This is expected because the monomers are equal in size and any other aspect except their reactivity. Clearly, the volume of the illuminated region has increased, which is because the network tends to swell. Further, the total volume fraction of monomer units of monomer 2 (incorporating both polymerized and unpolymerized units) is higher in the illuminated region than in the dark region, $\varphi_2^{\text{illum}}+\varphi_{p,2}^{\text{illum}}>\varphi_1^{\text{illum}}+\varphi_{p,1}^{\text{illum}}$. If the system were fixed now, i.e., very fast polymerization of the remaining monomer, this would also be the case for monomer units in the polymer film. If one calculates any more reaction and diffusion steps, this difference becomes even larger. In addition, the total volume of the illuminated regions is larger than that of the dark regions, $V^{\text{illum}}>V^{\text{dark}}$. Clearly, the monomer with the highest reactivity eventually has the highest concentration in the illuminated regions; the grating formation is reactivity driven.

The second case study (case II) illustrates the effects of size entropy. The following conditions apply: a 1:1 volume ratio mixture of a mono(meth)acrylate ($f_1=0$) and a di(meth)acrylate ($f_2=1$) monomer with a size ratio of $\nu_2:\nu_1=3:1$ with initially, $\varphi_1^{\text{illum}}=\varphi_1^{\text{dark}}=0.5$ and $\varphi_2^{\text{illum}}=\varphi_2^{\text{dark}}=0.5$ and $V^{\text{dark}}=V^{\text{illum}}=V_0$. Starting from $0.15V_0$ of polymer formed in the illuminated region, $R_2=2R_1$, and the initial volume ratio equal, the polymer consists of $0.05V_0$ of monomer 1 and $0.10V_0$ of monomer 2. The resulting chemical potentials are now different from the ones found for the previous case: -0.379 and -0.360 for those of Eq. (15) and -1.658 and -1.693 for those of Eq. (16).

In contrast to the case where the size ratio was 1:1, the sign of the differences of the chemical potentials between the illuminated and dark area is now reversed. Interestingly, the volume fraction of monomer 1 is now too low in the illuminated region and too high in the dark region. Solving for thermodynamic equilibrium results in: -0.368 for Eq. (17) and -1.670 for Eq. (18) and the following values:

$$\begin{aligned} &\varphi_1^{\text{illum}}=0.465, \quad \varphi_2^{\text{illum}}=0.420, \quad \varphi_{p,1}^{\text{illum}}=0.038,\\ &\varphi_{p,2}^{\text{illum}}=0.077, \quad \varphi_1^{\text{dark}}=0.494, \quad \varphi_2^{\text{dark}}=0.506, \end{aligned}$$

TABLE II. The size and crosslinking properties of the monomers.

	Monomer 1		Monomer 2	
Case	ν_1	f_1	ν_2	f_2
I	1	0	1	1
II	1	0	3	1
III	1	1	1	1

$$V^{\text{illum}} = 1.303V_0, \quad V^{\text{dark}} = 0.697V_0.$$

Now the ratio of monomer 1 to monomer 2 is not the same in both regions. This ratio is higher in the illuminated regions than in the dark regions. This result is in contrast to that of the proposed model of Van Nostrum[6] were the system always tries to obtain an equal ratio in both regions. The use of a chemical potential in the model favors the incorporation of short monomers in the regions that contain polymer. This effect is entropy driven. No physical interactions or dynamics are needed to explain the result. The relative increase in conformational degrees of freedom is higher for shorter molecules than for longer ones when transferred from the dark to the illuminated region.

Interestingly, now the total volume fraction of monomer 1 units, both in the monomeric and the polymeric state, is now larger than the total volume fraction of monomer 2 units in the illuminated regions, $\varphi_1^{\text{illum}} + \varphi_{p,1}^{\text{illum}} > \varphi_2^{\text{illum}} + \varphi_{p,2}^{\text{illum}}$. If the system were fixed now, this would also be the case for monomer units in the polymer film. Again for more reaction and diffusion steps, this difference becomes even larger. In addition, the total volume of the illuminated regions is larger than that of the dark regions, $V^{\text{illum}} > V^{\text{dark}}$. So, the result is now the same as in the case of the system of the Cl-monoacrylate and the Si-dimethacrylate or the system of the Cl-monoacrylate and the F-diacrylate of previous articles;[4,5] the less reactive smaller monomer has the higher volume fraction in the illuminated region, and the illuminated regions contain more material than the dark regions.

A third case study (case III) concerns the formation of a fully crosslinked polymer. The following conditions apply: a 1:1 volume ratio mixture of two di(meth)acrylate monomers ($f_1 = f_2 = 1$) with a size ratio of $\nu_2 : \nu_1 = 1:1$ and a reactivity ratio of $R_2 = 2R_1$. After the reaction step, the current chemical potentials are: -0.636 and -0.693 for Eq. (15) and -0.754 and -0.693 for Eq. (16). The volume fraction of monomer 1 is now too high in the illuminated region and too low in the dark region. Solving for thermodynamic equilibrium results in: -0.666 for those of Eq. (17) and -0.721 for those of Eq. (18) and the following values:

$$\varphi_1^{\text{illum}} = 0.436, \quad \varphi_2^{\text{illum}} = 0.414, \quad \varphi_{p,1}^{\text{illum}} = 0.050,$$

$$\varphi_{p,2}^{\text{illum}} = 0.100, \quad \varphi_1^{\text{dark}} = 0.514, \quad \varphi_2^{\text{dark}} = 0.486,$$

$$V^{\text{illum}} = 1.000V_0, \quad V^{\text{dark}} = 1.000V_0.$$

Now the ratio of monomer 1 to monomer 2 is the same in both regions. This is similar to the proposed model of Van Nostrum,[6] based on differences in reactivities only. After fixation, there are no difference in the total volume of the two regions, $V^{\text{illum}} = V^{\text{dark}}$ and the monomer with the highest reactivity has the highest volume fraction in the illuminated regions, $\varphi_2^{\text{illum}} + \varphi_{p,2}^{\text{illum}} > \varphi_1^{\text{illum}} + \varphi_{p,1}^{\text{illum}}$. The behavior sketched here, is the same as for the system of the F-diacrylate and the Si-dimethacrylate described in a previous article.[5]

These three case studies demonstrate that the static model predicts the general trends concerning the size entropy and crosslinking correctly. However, dynamic effects are not considered, which leads to the unsatisfying result that unlimited diffusion takes place to achieve thermodynamic equilibrium until the end of the illumination. As a result, the monomer volume fractions are constant within a given illuminated or dark region regardless of its dimension. In a real system, the diffusion coefficients drop significantly and thermodynamic equilibrium is not achieved, resulting in a different final monomer-unit distribution. In addition, the role that the magnitudes of the reaction rates and diffusion coefficients play, is unaccounted for. Closer resemblance in the final monomer volume fraction profiles is achieved with the dynamic model that incorporates diffusion coefficients and reaction rates.

IV. RESULTS OF THE DYNAMIC MODEL

A number of simulations with the dynamic reaction/diffusion model were made and then compared with nuclear microprobe measurements, which show fine structure in the lateral profile. For these systems, the reaction rate constants of the monomers were estimated from DSC measurements. With standard radical chain polymerization theory,[27] it was found that for pure Cl-monoacrylate, the rate constant at a UV source distance of 7.5 cm (2 mW/cm^2) with 0.5 mass % of photoinitiator (Irgacure 651) was $k_{\text{ov}}^{\text{DSC,Cl}} = 0.05 \pm 0.01\,\text{s}^{-1}$. For mixtures containing different monomer mixtures, the overall rate constant was determined by comparing the times where the conversion reaches its maximum. To convert these reaction rate constants of the DSC to those of the grating preparation process, a square root dependence on both the photo-initiator concentration and the UV light intensity was assumed.[27] Any effect due to the Trommsdorf effect and diffusion-limited propagation at higher conversions is ignored. In the grating preparation process, the intensity of the lamp is comparable to the DSC experiments.

The order of magnitude of the diffusion coefficient at zero degree of polymerization was estimated from diffusion profile measurements[28] and $D_s(0)$ is in the order of $10^{-6}\,\text{m}^2/\text{s}$ (see Sec. V). Assuming $K_2 = 0$ in Eq. (11), for simplicity, the only free fit parameter is then K_1, which represents the dependence of the diffusion coefficient on the degree of polymerization, i.e., the polymer volume fraction.

Figures 2(a) and 2(b) shows a measurement with the nuclear microprobe of a system containing a mono- and a diacrylate, i.e., a 1:6.7 mass ratio mixture of the Cl-monoacrylate and the F-diacrylate.[5] The total areal density is not a constant due to swelling and the mass fraction of the less reactive and considerably smaller monoacrylate is higher in the illuminated regions. Table III shows all parameters used to simulate a measurement with the mono- and the diacrylate monomer. From DSC, the overall reaction rate is estimated by $k_{\text{ov}}^{\text{grat}} = 0.016 \pm 0.003\,\text{s}^{-1}$. Assuming that the F-diacrylate has twice the reactivity of the Cl-monoacrylate, $R_2 = 2R_1$, and that the overall rate can be approximated by a weighted average over the initial molar fractions of 0.30 Cl-monoacrylate and 0.70 F-diacrylate, the reaction rate constants R_1 and R_2 in Table III are obtained.

In Figs. 2(a), 2(b) and 2(c), 2(d), the measurement and the simulation are compared. The data can be fitted nicely with $K_1 = 0.21$. Both the absolute areal densities and the

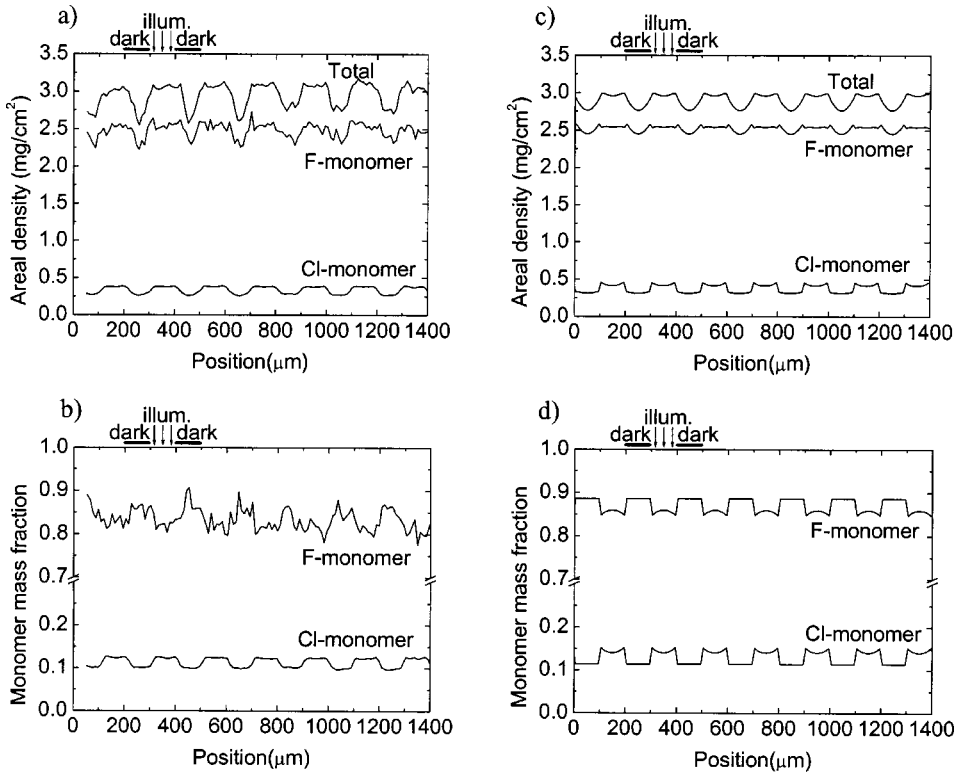

FIG. 2. Nuclear microprobe measurement (a) and (b) and simulation (c) and (d) of the total and the monomer areal densities and the monomer mass fractions of a mixture of the Cl-monoacrylate and the F-diacrylate.

monomer mass fractions are predicted correctly.

To stress the importance of the size ratio, another simulation is made with the same parameters except for the size ratio, which was changed from $\nu_1:\nu_2=1:3$ to 1:1. Figures 3(a) and 3(b) show that in this case the most reactive monomer is expected to migrate preferentially to the illuminated regions, which is not in agreement with the measurement of Figs. 2(a) and 2(b). In addition, the difference in total areal density is much less.

The dynamic model has several advantages over the static one. The monomer-unit volume fraction profiles of the final polymer structure can be determined quantitatively and directly compared with the nuclear microprobe measurements. From the dynamic model, it is concluded that even a ten times higher diffusion coefficient for the monoacrylate monomer in combination with a 1:1 volume ratio does not result in a higher monomer 1 volume fraction in the illuminated regions. The dynamic model also predicts that the high areal density regions are wider than the low areal density regions, as shown in Fig. 2(c). This is also observed in the measurement in Fig. 2(a). The dynamic model gives therefore a quantitative description of the reaction/migration process that includes experimental values of reaction/migration parameters.

The second system that is examined is the grating preparation of two di(meth)acrylate monomers. A 0.93:1 mixture

TABLE III. The parameters used for the simulation of a combination of the Cl-monoacrylate and the F-diacrylate for a UV light source distance of 20 cm. An approximate density of 1000 kg/m^3 is assumed to convert volume fraction directly in to mass fractions.

Reaction rate constants, etc.	$R_1=(0.9\pm0.2)\times10^{-2}\ \mathrm{s}^{-1}$	$\nu_1=1$	$f_1=0$
	$R_2=(1.8\pm0.4)\times10^{-2}\ \mathrm{s}^{-1}$	$\nu_2=3$	$f_2=1$
Diffusion coefficients	$D_1(0)=4.5\times10^{-10}\ \mathrm{m}^2/\mathrm{s}$	$K_1=0.21$	
	$D_2(0)=1.5\times10^{-10}\ \mathrm{m}^2/\mathrm{s}$	$K_2=0$	
	$D_s(0)=1.5\times10^{-6}\ \mathrm{m}^2/\mathrm{s}$	$\gamma=0.035\ \mathrm{J/m}^2$	
Initial values	$\varphi_1(x,0)=0.13$	Parameters for numerical	$t_{\max}=150$ s
	$h(x,0)=29.0\ \mu$m	calculation	$\Delta t=0.0125$ s
	$\lambda=200\ \mu$m		$L=20$
Cl-monoacrylate	$M_1=134.56$	Other parameters	$T=343$ K
	Cl mass per unit 35.453		$\nu_{\mathrm{segment}}=134\times10^{-6}\ \mathrm{m}^3$
F-diacrylate	$M_2=444.33$		
	F mass per unit 6×18.9984		

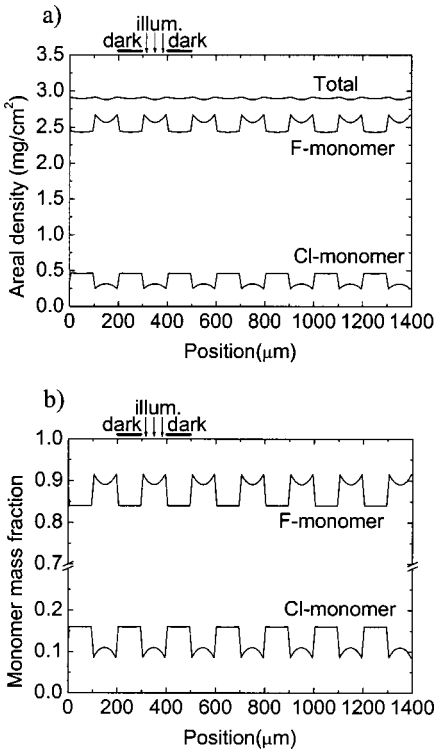

FIG. 3. Simulations of the total and the monomer areal densities of a mixture of the Cl-monoacrylate and the F-diacrylate, with a size ratio and 1:1 (a), and simulations of the monomer mass fractions, with a size ratio of 1:1 (b). In contrast to the measurement and the simulation of Figure 2, the F-diacrylate now has a higher mass fraction in the illuminated regions.

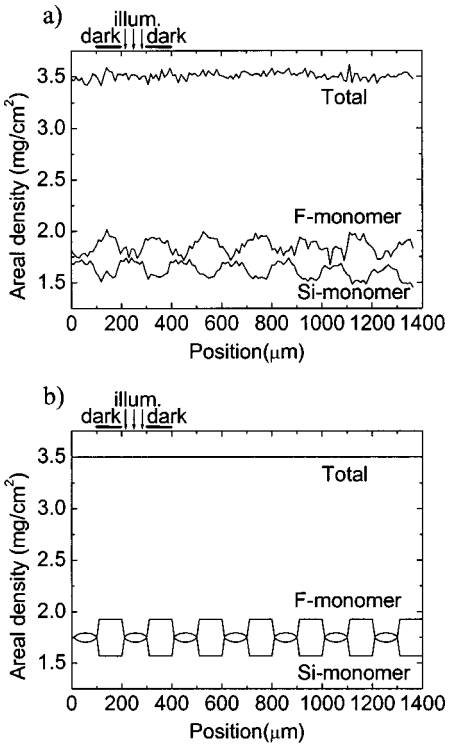

FIG. 4. Measurement (a) and simulation (b) of the total and the monomer areal densities of a grating prepared from a mixture of the Si-dimethacrylate and the F-diacrylate

of the F-diacrylate and the Si-dimethacrylate is used. This is the same system shown earlier in a previous article.[5] From DSC, the overall reaction rate constant is estimated to be $k_{ov}^{grat}=(3.9\pm0.8)\times10^{-3}\,s^{-1}$. The reaction rate constants R_1 and R_2 have been obtained by averaging over the molar fractions of 0.5 F-diacrylate and 0.5 Si-dimethacrylate and assuming a given value for R_2/R_1, in a similar way as for the previous case. Several values of R_2/R_1 were tried to obtain a good fit. The best fit was obtained for $R_2/R_1=1.22$. The corresponding rates and other parameters are displayed in Table IV.

A comparison between simulation and measurement is shown in Fig. 4. The difference between the areal densities of F and Si in the dark and illuminated regions of the simulation corresponds well with the nuclear microprobe measurement for the ratio of $R_2/R_1=1.22$. It is remarkable that changing the overall diffusion coefficient from 3×10^{-6} to $3\times10^{-9}\,m^2/s$ alters the volume fractions only by less than 0.1%. This can be understood since diffusion is only needed

TABLE IV. The parameters used for the simulation of a combination of the F-diacrylate and the Si-dimethacrylate. An approximate density of 1000 kg/m^3 is assumed to convert volume fraction directly in to mass fractions.

Reaction rate constants, etc.	$R_1=(3.5\pm0.7)\times10^{-3}\,s^{-1}$	$\nu_1=1$	$f_1=1$
	$R_2=(4.3\pm0.9)\times10^{-3}\,s^{-1}$	$\nu_2=1$	$f_2=1$
Diffusion coefficients	$D_1(0)=3.75\times10^{-10}\,m^2/s$	$K_1=0.16$	
	$D_2(0)=3.75\times10^{-10}\,m^2/s$	$K_2=0$	
	$D_s(0)=3.0\times10^{-6}\,m^2/s$	$\gamma=0.035$ J/m^2	
Initial values	$\varphi_1(x,0)=0.53$	Parameters for numerical	$t_{max}=450$ s
	$h(x,0)=35.0\ \mu$m	calculation	$\Delta t=2.5\times10^{-3}$ s
	$\lambda=200\ \mu$m		$L=20$
F-diacrylate	$M_1=444.33$	Other parameters	$T=343$ K
	F mass per unit 6×18.9984		$\nu_{segment}=400\times10^{-6}\,m^3$
Si-dimethacrylate	$M_2=386.64$		
	Si mass per unit 2×28.086		

to keep the total volume in the dark regions constant because there is no swelling.

V. DISCUSSION

For a combination of a 1:1 volume ratio mixture of two di(meth)acrylate monomers, with a size ratio of $\nu_2:\nu_1 = 1:1$ and a reactivity ratio of $R_2:R_1 = 2:1$, it was calculated with the static model that the maximum achievable volume ratio in the illuminated regions is about 60:40 at the end of the polymerization process when 90% of the illuminated region has been converted, which corresponds to a difference of 20% of the total volume between illuminated and dark regions. However, this assumes that at any time during the polymerization process, the system reaches thermodynamic equilibrium due to ''infinitely fast'' monomer diffusion. In a real system, due to decreasing diffusion coefficients as a function of conversion, the maximum difference is less than 20% and for better results the dynamic model should be considered.

Incorporation of a mono(meth)acrylate in a combination of a 1:1 volume ratio mixture with a di(meth)acrylate monomer with a size ratio of $\nu_2:\nu_1 = 1:1$ and a reactivity ratio of $R_2:R_1 = 2:1$, again results in a maximum difference of 20%. Altering the molecular sizes in a combination of a 1:1 volume ratio mixture of a mono(meth)acrylate and a di(meth)acrylate monomer with a size ratio of $\nu_2:\nu_1 = 3:1$ and a reactivity ratio of $R_2:R_1 = 2:1$, a maximum difference of only about 6% is found. For the latter two cases, both monomers flow to the illuminated regions in contrast to the system of the Si-dimethacrylate and the F-diacrylate, where counter diffusion was present. Note that a higher diffusion coefficient of one monomer can result in a more effective flow for this particular monomer. Therefore, in a real system, the actual difference can deviate from the calculated value.

As shown with the static model and the dynamic model, the size ratio $\nu_2:\nu_1$ is very important. For a combination of a di(meth)acrylate and a mono(meth)acrylate monomer, i.e., $R_2:R_1 = 2:1$, it was observed that if $\nu_2:\nu_1 = 1:1$, the monomer with the highest reactivity eventually has the highest concentration in the illuminated regions. For $\nu_2:\nu_1 = 3:1$, the monomer with the lowest reactivity has the highest concentration in the illuminated regions. As expected, somewhere between these two ratios of $\nu_2:\nu_1$, there should be a crossover point where both monomers have the same concentration in the illuminated and the dark regions. It can be expected that the interaction parameters χ_{ij}, which were assumed 0 in the model, determine the direction of flow in real systems if both reactivity and size entropy effects roughly cancel each other out. Although the dynamic reaction/diffusion model considers many aspects of polymer/monomer physics, two phenomena are not accounted for. First, phase separation is not treated, which is related with the fact that all interaction parameters are zero. For every interval Δx, it is assumed that the reacting system can be considered as one phase, i.e., all components are miscible. In the real case, this may not be true, e.g., when the system reaches a high monomer conversion. Then phase separation can occur within an interval Δx because the network does not dissolve in the remaining monomer. Second, at high degrees of polymerization, the polymer becomes glassy. Monomer diffusion becomes non-Fickian and must be described by case-II diffusion.[29] When the polymer is rubbery, the swelling occurs almost instantaneously. When, on the other hand, the polymer is glassy, the monomer first moves, creating a higher density, and swelling goes slowly.[30] However, at high conversions, the diffusion coefficients are very small anyway compared to ones during the early states of polymerization, and hardly any mass transport takes place. Therefore, since both phase separation of the polymer and case-II diffusion takes place at higher conversion, when most of the diffusion has already occurred, it is not considered to introduce large errors in the model. The high diffusion coefficients at the beginning of the polymerization process are dominant.

The number of crosslinks in the model, as a function of time (or conversion), has been adjusted in such a way that no swelling occurs for the system of two di(meth)acrylate monomers of the same size, at any value of time. It is hardly imaginable that the number of crosslinks indeed has this exact value to prevent the illuminated regions from swelling. The predicted number of crosslinks in the system of one crosslinking and one noncrosslinking monomer can therefore also deviate considerably from the one inserted in the model. Even better results are expected when the real crosslink density as a function of the time could be inserted. Furthermore, surface tension can also play an important role to prevent the system from swelling.

The most important input parameters of the model are the monomer reaction rate constants (s^{-1}), the diffusion coefficients and the monomer sizes, or more strictly the lengths of the monomers. The former ones were determined from DSC measurements. The initial monomer diffusion coefficients $D_1(0)$, $D_2(0)$ were determined from measurements of diffusion profiles.[28] The monomer sizes were estimated from calculated molecular conformations obtained form energy minimization.

Because all χ parameters are taken zero, and the overall mass diffusion coefficient is much larger than the diffusion coefficients of the monomers, which are in the order of $10^{-6}\,m^2/s$, the only parameters that are varied to fit the simulations with the measurements are the free volume parameters K_1 and K_2. For simplicity, K_2 is taken zero, which corresponds to an exponential decrease of the diffusion coefficient with degree of conversion. All microprobe measurements can already be satisfactorily simulated by only changing one parameter, K_1. It is possible to obtain similar simulations when increasing the initial diffusion coefficients and taking a lower value of K_1, indicating a faster decrease of the diffusion coefficients with conversion. This, however, can only be done within about one order of magnitude of the diffusion coefficients. For the F/Cl system, for instance, when the diffusion coefficients are increased by a factor of four, the K_1 value has to be changed from 0.21 to 0.16 to obtain a similar simulation.

The diffusion coefficients used in the model calculations at zero polymer volume fraction are all on the order of 10^{-9}–$10^{-10}\,m^2/s$. For comparison, the diffusion coefficients

of methylmethacrylate (MMA) in polymethylmethacrylate (PMMA) and polybutylmethacrylate (PBMA) are $D=2\times10^{-9}\,m^2/s$ (0% conversion) and $3\times10^{-10}\,m^2/s$ (50% conversion),[31,32] respectively. For high conversion, the diffusion coefficient of MMA in PMMA is $2\times10^{-14}\,m^2/s$ at $T=150\,°C$.[33] The diffusion coefficient of methanol, another small molecule, in PMMA is $10^{-14}\,m^2/s$ at $T=24\,°C$.[29] The diffusion coefficients for several acrylate monomers can drop up to 5 orders of magnitude, e.g., from $10^{-11}\,m^2/s$ at 0% polymerization to $10^{-16}\,m^2/s$ at 100% polymerization.[19]

Considering the grating prepared from the F-diacrylate and Cl-monoacrylate monomers, it is interesting to note that for the simulations with the dynamic model, the obtained values of $K_1=0.21$ and $K_2=0$ indicate that the diffusion coefficients drop by 1 order of magnitude, going from 0% polymer to 50% polymer. This corresponds nicely with the behavior of MMA in PMMA and PBMA, which also drops by 1 order of magnitude:[31,32] $D\approx2\times10^{-9}\,m^2/s$ (0% conversion) and $D\approx3\times10^{-10}\,m^2/s$ (50% conversion). The value of K_1 is lower for the system of the Si-dimethacrylate and the F-diacrylate ($K_1=0.16$), which indicates a steeper decrease for increasing polymer volume fraction. This is to be expected since the Si–F system has a higher crosslinking density than the previous F–Cl system since both monomers are di(meth)acrylate. More indications of diffusion coefficients are found in the literature:[21,34] a hexafunctional oligomer ($M=1000$): $D=10^{-15}\,m^2/s$ (unpolymerized), a trifunctional oligomer ($M=2300$): $D=0.5\times10^{-15}\,m^2/s$ (unpolymerized), the liquid crystal BL038 in an oligomer mixture: $D=10^{-11}\,m^2/s$ (unpolymerized), camphorquinone in polybutadiene: $D=10^{-17}-10^{-16}\,m^2/s$, and photoproduct of camphorquinone in PMMA of low molecular weight: $D=10^{-17}-10^{-16}\,m^2/s$. Hence, although the description of the diffusion coefficients is rather rough, by assuming a certain value at zero conversion and an exponential decrease as a function of conversion, the values correspond reasonably well with values in the literature.

The value of $D_s(0)$ is on the order of $10^{-6}\,m^2/s$ for all systems. This value corresponds with the following rough estimate based on fluid mechanics. In general, the treatment of flow of a liquid, with a liquid–vapor interface on top, is quite complex when surface tension plays a role.[35] Here, a somewhat simplified picture is presented. For the laminar flow of a liquid of height h driven by a certain pressure gradient, and an interface of the liquid with air on top, the flux of particles per unit area j ($m^3\,s^{-1}\,m^{-2}$) is given by

$$j=-\frac{1}{3}\frac{1}{\eta}\frac{dp}{dx}h^2,$$

which can be found in any literature about fluid mechanics. In the case of a laminar flow between two parallel plates, the prefactor $\frac{1}{3}$ has to be changed to $\frac{1}{12}$. A pressure gradient Δp in the x direction is equivalent to an overall chemical potential gradient $\Delta\overline{\mu}/\nu_{\text{segment}}$, where the chemical potential is averaged over the height and ν_{segment}, as in Eq. (12), is the volume of migrating species. This flux is also given by $j=-(D_s/kT)(d\mu_s/dx)$ from Eq. (13). Because the chemical potential in the reaction/diffusion model is treated as a constant in every column of height h, and the surface chemical potential only applies to the outmost layer of segments of volume ν_{segment}, the following conversion is needed, where r is the Van der Waals or Stokes radius of the migrating species: $\overline{\mu}\approx\mu_s(2r/h)$. With the considerations discussed here, Eq. (13), and assuming spherical segments, i.e., $\nu_{\text{segment}}=4\pi r^3$, with a radius r of about 1 nm, a viscosity η equivalent of that of water (1 m Pa s) and a height h of 25 μm, this results in $D_s(0)\approx5\times10^{-6}\,m^2/s$. This rough estimate justifies the values for this diffusion coefficient in the model, since it is of the same order. Moreover, since D_s, D_1, and D_2 are all inversely proportional to the viscosity η, the same exponential dependence on the polymer volume fraction, given by Eq. (11), is expected.

Several important aspects concerning two-way diffusion or one-way diffusion are predicted correctly by the model. It correctly predicts the fact that, not only reactivity but also monomer size determines which monomer flows towards the illuminated regions and which flows to the dark. Moreover, a treatment that only uses concentrations as the driving force is unable to correctly predict the fact that less reactive small monomers flow towards the illuminated regions, as observed in numerous measurements. Entropically, it is more favorable to put a number of small molecules in a polymer network than fewer large molecules with the same volume.

In addition, the model stresses the importance of crosslinks with respect to the swelling of growing polymer in the illuminated regions. It correctly predicts swelling of the illuminated regions, in the case a considerable amount of noncrosslinking monomers is used. So, although the model contains some approximations and simplifications, the experimental data can be fitted very neatly with reasonable values of the reaction rate constants and monomer diffusion coefficients for low degrees of polymerization when comparing these values with values in literature.

VI. CONCLUSIONS

A model has been developed which uses the Flory–Huggins theory to describe the preparation process of polymer gratings by patterned UV photopolymerization of a mixture of two monomers. The reaction/diffusion mechanism is described using the chemical potential of the monomers in both the illuminated and the dark regions. The chemical potential incorporates the monomer volume fraction, which is determined by the reactivity, the monomer size, the crosslinking ability, and the monomer/monomer and monomer/polymer interaction.

A static model is easily derived from the description above. After every reaction step, considering the relative reaction rate constants of the two monomers, the monomers are redistributed in such a way that thermodynamic equilibrium is reestablished. The outcome of the static model is consistent with the nuclear microprobe measurements done on gratings.[4,5] It is shown that, if monomers of the same size are used, the monomer with the highest reactivity eventually has the higher concentration in the illuminated regions. However, the chemical potential both incorporates the volume fraction and the monomer size. It is entropically more favorable to store a large number of smaller monomers in the

partly polymerized illuminated regions than a smaller number of larger monomers with the same total volume. Thus, not only with increasing reactivity but also with decreasing monomer size, the tendency to migrate to the illuminated regions increases.

In addition, the model describes the swelling of polymer formed in the illuminated regions. Polymer swelling is entropically favorable because the number of possible configurations increases. However, when the polymer is crosslinked, the number of configurations of the polymer decreases, which is entropically unfavorable. The balance between these two effects determines the amount of swelling of the illuminated regions. In the model, the number of crosslinks determines the strength of the network. Because this quantity is not measured, it is chosen to adjust this value to the one that does not result in swelling for two crosslinking monomers. For a combination of other monomers, only a fraction of this quantity is used, proportional to the volume fraction of the crosslinking monomer.

However, the static model also has severe limitations. First, no dynamics are involved. In a real system, it is not possible that the monomers migrate so fast that thermodynamic equilibrium is maintained. Especially, when the degree of polymerization becomes higher, the system is ''diffusion limited.'' The final monomer-unit distribution cannot be determined. In addition, monomer volume fractions are constant within the illuminated and dark region, which does not correspond to reality. Second, it is assumed that the illuminated region can swell unlimitedly. In the dynamic model discussed hereafter, both a surface tension term, reaction rate constants and diffusion coefficients are incorporated.

By adding diffusion equations to the static model, a dynamic model is established. The monomer diffusion is driven by a gradient in chemical potential, which is fundamentally more correct than the empirical Fick's second law. In addition, a migration coefficient driven by surface tension is added, which works on both monomers equally.

By inserting reaction rate constants obtained from DSC, estimations of the monomer size, and the experimentally measured diffusion coefficients[28] into the dynamic reaction/diffusion model, simulations for some combinations of mono- and di(meth)acrylate monomers are obtained. These simulations of the final monomer-unit distributions correspond very well with nuclear microprobe measurements. It correctly predicts which monomer unit eventually has the highest volume fraction in the illuminated regions.

Despite the many approximations, the experimental data fit very neatly with values for the monomer diffusion coefficients and reaction rate constants that are reasonably in agreement with those in literature. The model contributes in the understanding of monomer diffusion processes during photopolymerization processes where the reaction rate constant depends on the position in the monomer mixture.

APPENDIX A: NUMERICAL PROCEDURE FOR A STATIC REACTION/DIFFUSION MODEL

With the theory sketched above, it is possible to set up a static reaction/diffusion model. In the static model, the system is divided into two regions, the illuminated and the dark area. After a certain amount of polymer is formed and taking the reactivity of the two monomers into account, the chemical potentials of the monomers in the dark and the illuminated region are calculated. Subsequently, the volume fractions at thermodynamic equilibrium are determined. This is done by redistributing the mobile monomers over the two regions and demanding that the chemical potentials of the monomers are equal in both regions. This is equivalent to minimizing the total free energy of the whole system. These volume fractions are taken as their new values and the process is repeated by converting again some monomer into polymer. In the rest of the section, this is discussed in more detail. The whole procedure is summarized in Fig. 1.

Initially, the same volume fractions in both the illuminated and the dark region are present: $\varphi_1^{\text{illum}}=\varphi_1^{\text{dark}}$ and $\varphi_2^{\text{illum}}=\varphi_2^{\text{dark}}$. The total volumes of the two regions are also equal: $V^{\text{illum}}=V^{\text{dark}}=V_0$. Subsequently, in the model a certain volume of monomers in the illuminated region is converted into polymer. The reactivity ratio R_1/R_2 together with the volume fractions of available monomers $\varphi_1^{\text{illum}}/\varphi_2^{\text{illum}}$ determines how much of the converted polymer volume is formed from monomer 1 or monomer 2

$$\varphi_p^{\text{illum}}=\varphi_{p,1}^{\text{illum}}+\varphi_{p,2}^{\text{illum}} \quad \text{with} \quad \frac{\varphi_{p,1}^{\text{illum}}}{\varphi_{p,2}^{\text{illum}}}=\frac{R_1\varphi_1^{\text{illum}}}{R_2\varphi_2^{\text{illum}}}. \tag{A1}$$

Here, $\varphi_{p,i}^{\text{illum}}$ is the volume fraction of polymer originating from monomer i, i.e., the volume fraction of polymerized monomer i. In the dark regions, $\varphi_p^{\text{dark}}=0$ at all times. After this, the crosslink density is determined. From measurements,[4,5] no swelling is observed, for (a combination of) di(meth)acrylate monomers. To incorporate this in the model, n_e is adjusted in such a way that no swelling occurs for crosslinking monomers at any stage in the polymerization process. If there were only one monomer species, the following value for the chain density n_e/N_p, which is the equivalent of equation 5, would be the value that would give no swelling:

$$\frac{n_e}{N_p}=\frac{1}{\nu_1}\frac{-\ln(1-\varphi_p^*)-\varphi_p^*}{\left(\frac{1}{\varphi_p^*}-\frac{\varphi_p^*}{2}\right)}. \tag{A2}$$

Here, φ_p^* is the polymer volume fraction, calculated from the volume of polymer, assuming a total volume of V_{initial}

$$\varphi_p^*=\varphi_p^{\text{illum}}\frac{V^{\text{illum}}}{V_{\text{initial}}}. \tag{A3}$$

It should be noted that contributions due to entanglements of polymer chains are not taken into account in the Flory–Huggins treatment, and the effective value of n_e/N_p will be higher than the one calculated from the physical number of crosslinks.[9]

If two monomers are used, the chain density is assumed to be the weighted average over the two monomers

$$\frac{n_e}{N_p}=\frac{1}{\varphi_p^{\text{illum}}}\left(f_1\frac{\varphi_{p,1}^{\text{illum}}}{\nu_1}+f_2\frac{\varphi_{p,2}^{\text{illum}}}{\nu_2}\right)\frac{-\ln(1-\varphi_p^*)-\varphi_p^*}{\left(\frac{1}{\varphi_p^*}-\frac{\varphi_p^*}{2}\right)}. \tag{A4}$$

Here, f_1 equals either unity [if monomer 1 is a di(meth)acrylate (i.e., crosslinking) monomer] or zero [if it is a mono(meth)acrylate (i.e., noncrosslinking) monomer]. The same holds for f_2. $\varphi_{p,1}^{\text{illum}}$ and $\varphi_{p,2}^{\text{illum}}$ are the volume fractions of polymerized monomer 1 and 2, respectively. So, $\varphi_p^{\text{illum}}=\varphi_{p,1}^{\text{illum}}+\varphi_{p,2}^{\text{illum}}$. In the case of two di(meth)acrylate monomers of equal size, the formula reduces again to Eq. (A2). So the crosslink density is calculated by Eq. (A4) and chemical potential of the monomers in both the illuminated and the dark area are determined with Eqs. (6) and (7).

The unreacted monomers are then redistributed over both regions in such a way that the chemical potential in the illuminated region for each monomer is equal to the corresponding one in the dark area. It is noted that the total volumes of both regions are not constants and overall mass transport to one region is allowed and that the segments are assumed to be incompressible. In this way, a new set of equilibrium values of φ_1^{illum}, φ_1^{dark}, φ_2^{illum}, φ_2^{dark}, V^{illum}, and V^{dark} is created. It is clear, due to conservation of mass, that these values are not independent. For instance, $V^{\text{dark}}=2V_0-V^{\text{illum}}$. The model can be made semidynamic by starting from the end situation calculated above and repeating the procedure. Again, some monomer is converted into polymer according to their reactivity ratio, after which the monomers are redistributed to obtain thermodynamic equilibrium. It this way, one can proceed until a conversion of about 90% is reached in the illuminated regions. The size of the reaction steps can be changed. The fixation step of the grating preparation process is represented simply by converting all the remaining monomer into polymer without any redistribution. In this way, it is possible to calculate the final composition of the grating. Because this model uses thermodynamic equilibrium only, no dynamics or time scales are involved. However, it clearly shows the migration direction of the monomers, when the system is partly polymerized, and whether the illuminated regions swell or not due to overall material transport. It is also useful to determine the fundamental limit of the volume fraction difference between the two regions under the condition that the conversion step size is sufficiently small.

APPENDIX B: NUMERICAL PROCEDURE FOR A DYNAMIC REACTION/DIFFUSION MODEL

To predict which monomer flows to the illuminated regions, it is necessary to write down the chemical potentials of these monomers in both the illuminated and the dark regions as was done for the static model. There the system was split up in two phases. On one side, there was the liquid, on the other side the mixture of monomer and polymer. Now, the grating pitch λ, consisting of one illuminated and one dark area, is split up in a number of regions L with length of Δx. The volume of such a region V is given by $\Delta x\Delta y\, h$ with h the height of the layer. The value of Δy does not influence the simulation. At each position, the local chemical potential for each monomer can be expressed as a function of the monomer and polymer volume fractions and the number of crosslinks, in a similar way as done in Eqs. (6) and (7). At $t=0$, the volume of each region is the same, $V(x,0)=V_{\text{initial}}$. Monomer reaction is represented by the following equations:

$$V_{m,i}(x,t+\Delta t)=V_{m,i}(x,t)-R_iV_{m,i}(x,t)\Delta t, \tag{B1}$$

$$V_{p,i}(x,t+\Delta t)=V_{p,i}(x,t)+R_iV_{m,i}(x,t)\Delta t. \tag{B2}$$

Here $V_{m,i}(x,t)$ is the volume of monomer i and $V_{p,i}$ is the volume of polymerized monomer i at position x and time t. R_i is the reaction rate constant in s^{-1}. For each region of length Δx, the monomer chemical potentials are given by Eqs. (6) and (7), still assuming zero interaction parameters ($\chi_{ij}=0$ for all i, j) and $\nu_1\ll\nu_p$ and $\nu_2\ll\nu_p$. So, for regions with polymer, with $N_p=V\varphi_p/\nu_{\text{segment}}$, with ν_{segment} the volume of a segment (m^3), the chemical potentials of monomer 1 for a position x and time t is given by

$$\mu_1(x,t)-\mu_1^0=kT\left[\ln\varphi_1(x,t)+1-\varphi_1(x,t)-\frac{\nu_1}{\nu_2}\varphi_2(x,t)+\nu_1\frac{n_e(x,t)\nu_{\text{segment}}}{V(x,t)\varphi_p(x,t)}\left(\frac{1}{\varphi_p(x,t)}-\frac{\varphi_p(x,t)}{2}\right)\right] \tag{B3}$$

for $x\in$ illuminated regions.

For regions without polymer, the last term is equal to zero, and the expressions for the chemical potential reduce to

$$\mu_1(x,t)-\mu_1^0=kT\left[\ln\varphi_1(x,t)+1-\varphi_1(x,t)-\frac{\nu_1}{\nu_2}\varphi_2(x,t)\right] \tag{B4}$$

for $x\in$ dark regions. The chemical potential of the polymer needs not to be considered, because the polymer is assumed immobile on the time scale of our diffusion experiments. For monomer 2, similar expressions are found by exchanging the indices 1 and 2.

Again as for the static model, n_e is adjusted in such a way that no swelling occurs for crosslinking monomers for all values of x and t. For only one monomer species, the following value for n_e, which is the equivalent of Eq. (A2), would be the value that would give no swelling:

$$n_e(x,t)=\varphi_p(x,t)V(x,t)\frac{1}{\nu_1\nu_{\text{segment}}}\times\frac{-\ln(1-\varphi_p^*(x,t))-\varphi_p^*(x,t)}{\left(\frac{1}{\varphi_p^*(x,t)}-\frac{\varphi_p^*(x,t)}{2}\right)}. \tag{B5}$$

Here, φ_p^* is the polymer volume fraction assuming a volume of V_{initial}

$$\varphi_p^*(x,t)=\varphi_p(x,t)\frac{V(x,t)}{V_{\text{initial}}}. \tag{B6}$$

If two monomers are used, the chain density is represented by a weighted average over the expression of Eq. (B5) for the two monomers

$$n_e(x,t)=\frac{V(x,t)}{\nu_{\text{segment}}}\left(f_1\frac{\varphi_{p,1}(x,t)}{\nu_1}+f_2\frac{\varphi_{p,2}(x,t)}{\nu_2}\right)\times\frac{-\ln(1-\varphi_p^*(x,t))-\varphi_p^*(x,t)}{\left(\frac{1}{\varphi_p^*(x,t)}-\frac{\varphi_p^*(x,t)}{2}\right)}. \tag{B7}$$

Here, f_1 equals either unity if monomer 1 is a di(meth)acrylate (i.e., crosslinking) monomer or zero if it is a mono(meth)acrylate (i.e., noncrosslinking) monomer. The same holds for f_2. $\varphi_{p,1}$ and $\varphi_{p,2}$ are the volume fractions of polymerized monomer 1 and 2, respectively. So, $\varphi_p=\varphi_{p,1}+\varphi_{p,2}$. In the case of two di(meth)acrylate monomers of equal size, the formula reduces again to Eq. (B5).

The diffusion coefficients of the monomers $i=1$, 2 decrease as a function of polymer volume fraction and are determined with

$$D_i(x,t)=D_i(0)\exp\left(-\frac{1}{K_1(1+K_2)}\right)\times\exp\left(\frac{1}{K_1\left(\frac{1}{1-\varphi_p(x,t)}+K_2\right)}\right). \tag{B8}$$

Here $D_i(0)$ is the diffusion coefficient of monomer i when there is no polymer, i.e., $\varphi_p=0$, and K_1 and K_2 are constants from the free volume theory [Eq. (11)]. With Eq. (10), the discretized diffusion equations for monomers 1 and 2 result in Eq. (B9) for monomers $i=1$, 2. Conservation of mass requires the use of $V_{m,i}$ instead of c.

$$V_{m,i}(x,t+\Delta t)=\left\{V_{m,i}(x,t)+\Delta t\left(\frac{1}{2}\frac{D_i(x,t)V_{m,i}(x,t)}{kT(\Delta x)^2}[\mu_i(x-1,t)-2\mu_i(x,t)+\mu_i(x+1,t)]+\frac{1}{2}\frac{D_i(x-1,t)V_{m,i}(x-1,t)}{kT(\Delta x)^2}\times[\mu_i(x-1,t)-\mu_i(x,t)]+\frac{1}{2}\frac{D_i(x+1,t)V_{m,i}(x+1,t)}{kT(\Delta x)^2}[\mu_i(x+1,t)-\mu_i(x,t)]\right)\right\}. \tag{B9}$$

With the discretized version of Eq. (12), and ν_{segment} as the unit of the migrating species, the surface energy chemical potential is given by

$$\mu_s(x,t)=-\gamma\nu_{\text{segment}}\left[\frac{\frac{1}{(\Delta x)^2}[h(x-1,t)-2h(x,t)+h(x+1,t)]}{\left(1+\left(\frac{1}{\Delta x}[h(x+1,t)-h(x-1,t)]\right)^2\right)^{3/2}}\right]. \tag{B10}$$

Here h is the height of the mixture. With the discretized version of Eq. (13), the change of the total volume due to total mass transport is given by Eq. (B11). $V_{m,i}$ is used instead of n.

$$V_{m,i}(x,t+\Delta t)=\left\{V_{m,i}(x,t)+\Delta t\left(\frac{1}{2}\frac{D_i(x,t)V_{m,i}(x,t)}{kT(\Delta x)^2}[\mu_s(x-1,t)-2\mu_s(x,t)+\mu_s(x+1,t)]+\frac{1}{2}\frac{D_i(x-1,t)V_{m,i}(x-1,t)}{kT(\Delta x)^2}\times[\mu_s(x-1,t)-\mu_s(x,t)]+\frac{1}{2}\frac{D_i(x+1,t)V_{m,i}(x+1,t)}{kT(\Delta x)^2}[\mu_s(x+1,t)-\mu_s(x,t)]\right)\right\}. \tag{B11}$$

[1] H. J. Lee, M. H. Lee, M. C. Oh, J. H. Ahn, and S. G. Han, J. Polym. Sci., Part A: Polym. Chem. **37**, 2355 (1999).
[2] M. Kagami, A. Kawasaki, and H. Ito, J. Lightwave Technol. **19**, 1949 (2001).
[3] G. J. Steckman, R. Bittner, K. Meerholz, and D. Psaltis, Opt. Commun. **185**, 13 (2000).
[4] C. M. Leewis, D. P. L. Simons, A. M. de Jong, D. J. Broer, and M. J. A. de Voigt, Nucl. Instrum. Methods Phys. Res. B **161–163**, 651 (2000).
[5] C. M. Leewis, P. H. A. Mutsaers, A. M. de Jong, L. J. van IJzendoorn, D. J. Broer, and M. J. A. de Voigt, Nucl. Instrum. Methods Phys. Res. B **181**, 367 (2001).
[6] C. F. van Nostrum, R. J. M. Nolte, D. J. Broer, Th. Fuhrman, and J. H. Wendorff, Chem. Mater. **10**, 135 (1998).
[7] G. M. Karpov, V. V. Obukhovsky, T. N. Smirnova, and V. V. Lemeshko, Opt. Commun. **174**, 391 (2000).
[8] S. Piazzolla and B. K. Jenkins, Opt. Lett. **21**, 1075 (1996).
[9] P. J. Flory, *Principles of Polymer Chemistry* (Cornell University Press, Ithaca, N.Y., 1953).
[10] R. A. L. Jones and R. W. Richards, *Polymers at Surfaces and Interfaces* (Cambridge University Press, Cambridge, MA, 1999).
[11] T. L. Hill, *An Introduction to Statistical Thermodynamics* (Addison-Wesley, London, 1960).
[12] H. S. Han and K. A. Dill, J. Chem. Phys. **101**, 7007 (1994).
[13] G. W. H. Höhne, W. Hemminger, and H. J. Flammersheim, *Differential Scanning Calorimetry, An Introduction for Practioners* (Springer, Berlin, 1996).
[14] N. L. Thomas and A. H. Windle, Polymer **22**, 627 (1981).
[15] J. J. Hermans, J. Polym. Sci. **59**, 191 (1962).
[16] P. J. Flory, Proc. R. Soc. London, Ser. A **351**, 351 (1976).
[17] A. W. Adamson and A. P. Gast, *Physical Chemistry of Surfaces* (Wiley, Chichester, 1997).

[18] P. W. Atkins, *Physical Chemistry*, 6th ed. (Oxford University Press, Oxford, 1998).
[19] R. H. Wopschall and T. R. Pampalone, Appl. Opt. **11**, 2096 (1972).
[20] V. L. Colvin, R. G. Larson, A. L. Harris, and M. L. Schillings, J. Appl. Phys. **81**, 5913 (1997).
[21] J. Xia and C. H. Wang, J. Polym. Sci., Part B: Polym. Phys. **33**, 899 (1995).
[22] H. Fujita and A. Kishimoto, J. Chem. Phys. **34**, 393 (1961).
[23] J. Crank, *The Mathematics of Diffusion*, 2nd ed. (Oxford University Press, Oxford, 1990).
[24] L. B. Freund, Int. J. Solids Struct. **32**, 911 (1995).
[25] *Chambers Science and Technology Dictionary*, edited by P. M. B. Walker (Chambers, Cambridge, MA, 1988).
[26] ⟨www.sartomer.com⟩
[27] G. Odian, *Principles of Polymerization* (McGraw–Hill, New York, 1970).
[28] C. M. Leewis, P. H. A. Mutsaers, A. M. de Jong, L. J. van IJzendoorn, M. J. A. de Voigt, M. Q. Ren, F. Watt, and D. J. Broer, J. Chem. Phys. **120**, 1820 (2004).
[29] N. L. Thomas and A. H. Windle, Polymer **23**, 529 (1982).
[30] C. Y. Hui, K. C. Wu, R. C. Lasky, and E. J. Kramer, J. Appl. Phys. **61**, 5137 (1987).
[31] M. P. Tonge and R. G. Gilbert, Polymer **42**, 1393 (2001).
[32] M. C. Griffiths, J. Strauch, M. J. Monteiro, and R. G. Gilbert, Macromolecules **31**, 7835 (1998).
[33] G. Compagnini, G. G. N. Angilella, A. Raudino, and O. Puglisi, Nucl. Instrum. Methods Phys. Res. B **175–177**, 559 (2001).
[34] C. C. Bowley and G. P. Crawford, Appl. Phys. Lett. **76**, 2235 (2000).
[35] F. M. White, *Viscous Fluid Flow* (McGraw–Hill, New York, 1974).